Relative Rates and Potentials of Competing Redox Processes during DNA Cleavage: Oxidation Mechanisms and Sequence-Specific Catalysis of the Self-Inactivation of Oxometal Oxidants by DNA

Chien-Chung Cheng, James G. Goll,† Gregory A. Neyhart, Thomas W. Welch, Phirtu Singh, and H. Holden Thorp*

Contribution from the Department of Chemistry, University of North Carolina, Chapel Hill, North Carolina 27599-3290

Received August 18, 1994®

Abstract: The redox reactions of the isostructural complexes $Ru(tpy)(bpy)O^{2+}$, $Ru(tpy)(bpy)OH^{2+}$, and $Os(tpy)(bpy)O^{2+}$ with DNA have been investigated (tpy = 2,2″-terpyridine, bpy = 2,2′-bipyridine). The Ru(IV) complex, which is a two-electron oxidant, cleaves DNA by sugar oxidation at the 1′ position, which is indicated by the termini formed with and without piperidine treatment and by the production of free bases and 5-methylene-2(5*H*)-furanone. This sugar oxidation occurs in the minor groove, as indicated by the inhibition of the reaction by distamycin. The Ru(IV) complex also oxidizes guanine bases to produce piperidine-labile cleavages. Densitometry and product analysis indicate that about 20% of the metal complex is reduced via the sugar oxidation pathway and about 30% via the base oxidation pathway. The Ru(III) complex is a one-electron oxidant but can access a two-electron pathway via an unfavorable disproportionation to Ru(IV). The Ru(III) complex cleaves DNA only by guanine oxidation, which is consistent with the higher yield of base oxidation relative to sugar oxidation observed for Ru(IV). The Os(IV) complex is a weaker one-electron oxidant. As a result, the Os(IV) complex cleaves DNA in supercoiled plasmids, but no cleavages have been detected in single- or double-stranded oligomers. Nonetheless, the reduction of the Os(IV) complex is significantly faster in the presence of DNA than in buffer, suggesting that the DNA is catalyzing a self-inactivation reaction of the oxometal oxidant. These self-reduction pathways are known for related oxidants and presumably account for the remainder of the Ru(IV) oxidant not apparent on sequencing gels. Further, the DNA catalysis is sequence-specific, which may have profound implications for understanding the cleavage patterns of many oxometal oxidants.

The oxidative damage of DNA by metal complexes is of interest in pharmaceutical applications and in developing probes for nucleic acid structure in solution.[1-3] Because of recent advances in experimental methodology, it has become possible to begin understanding the mechanisms of DNA cleavage on a fundamental level.[4,5] For example, cleavage of DNA by bleomycin (BLM) has been shown to occur via activation of oxygen by Fe(II)BLM to form a high-valent species (activated BLM) that is capable of abstracting the 4′-hydrogen atom from DNA sugars. Activated BLM is also capable of self-inactivation, as indicated by the fact that repeated electrochemical activation in the absence of DNA leads to a dramatic loss in the ability of BLM to degrade DNA.[6] The presence of DNA protects BLM from self-inactivation, leading to catalytic DNA damage; however, electrochemical experiments show a decrease in catalytic current during electrochemically activated DNA degradation,[6] indicating that self-inactivation does compete with DNA cleavage to some extent. This self-reduction process is reminiscent of the suicide inactivation of oxidized cytochrome P-450 and heme analogs by certain substrates.[7]

Recent studies have shown that sequence-specific isotope effects are observed for cleavage by FeBLM.[8,9] The isotope effects are observed by selective incorporation of 4′-deuterated nucleotides in restriction fragments and comparison of the extent of cleavage for the deuterated versus unlabeled sites. The observation of such a net isotope effect is revealing with regard to the cleavage mechanism. The first step in cleavage of DNA by activated FeBLM involves binding of the activated complex to DNA. As shown in Scheme 1, the bound complex can then either cleave DNA ($k_{cleavage}$), dissociate (k_{off}), or undergo other non-productive processes such as self-inactivation (k_X). The observation of a significant isotope effect on cleavage demonstrates that cleavage must be much slower than the other processes ($k_X + k_{off}$).[9] If this was not the case, then cleavage would be observed regardless of whether a hydrogen or deuterium was abstracted.

An important point brought out by Worth et al. is that the observed isotope effect $^D(V/K)$ is a net effect determined by the relative yields on a sequencing gel of cleavage of the protio and deuterio DNA.[9] This result must be considered in light of selection against other processes, so the apparent isotope effect is equal to the true kinetic isotope effect scaled by the rates of competing processes:

$$^D(V/K) = (k_H/k_D)[(k_D + k_X + k_{off})/(k_H + k_X + k_{off})] \quad (1)$$

† Present address: Department of Chemistry, University of Pennsylvania, Philadelphia, PA 19104.

® Abstract published in *Advance ACS Abstracts*, March 1, 1995.

(1) Sigman, D. S.; Bruice, T. W.; Mazumder, A.; Sutton, C. L. *Acc. Chem. Res.* **1993**, *26*, 98.
(2) Pyle, A. M.; Barton, J. K. *Prog. Inorg. Chem.* **1990**, *38*, 413.
(3) Burkhoff, A. M.; Tullius, T. D. *Nature (London)* **1988**, *331*, 455. Riordan, C. G.; Wei, P. *J. Am. Chem. Soc.* **1994**, *116*, 2189−2190.
(4) Hecht, S. M. *Acc. Chem. Res.* **1986**, *19*, 83.
(5) Stubbe, J.; Kozarich, J. W. *Chem. Rev.* **1987**, *87*. 1107.
(6) Van Atta, R. B.; Long, E. C.; Hecht, S. M.; van der Marel, G. A.; van Boom, J. H. *J. Am. Chem. Soc.* **1989**, *111*, 2722.
(7) Collman, J. P.; Hampton, P. D.; Brauman, J. I. *J. Am. Chem. Soc.* **1990**, *112*, 2977−2986.
(8) Kozarich, J. W.; Worth, L., Jr.; Frank, B. L.; Christner, D. F.; Vanderwall, D. E.; Stubbe, J. *Science* **1989**, *245*, 1396.
(9) Worth, J. L.; Frank, B. L.; Christner, D. F.; Absalon, M. J.; Stubbe, J.; Kozarich, J. W. *Biochemistry* **1993**, *32*, 2601.

0002-7863/95/1517-2970$09.00/0

Scheme 1

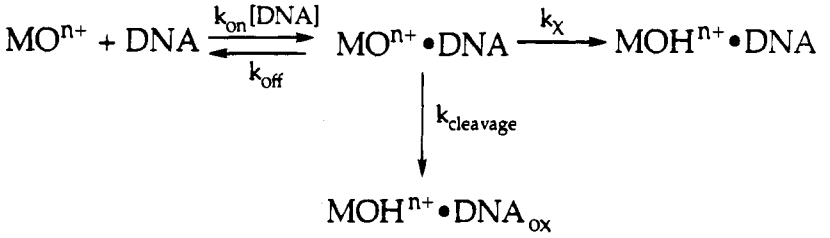

The observed isotope effects are sequence-specific, which could result either from different transition-state geometries for hydrogen abstraction at different sites (i.e. different k_H/k_D) or from a dependence of k_X (or k_{off}) on the DNA sequence. We report here on a system that exhibits such a sequence-specific k_X.

One of the goals of our research program has been to develop systems where the dynamics in Scheme 1 can be studied in real time with complexes that exhibit unique spectroscopic signatures. In addition, modulation of the reactivity of the cleavage agent may ultimately allow us to effect predictable changes in the cleavage selectivity because of changes in the relative rates of the processes shown in Scheme 1. To this end, we have developed new DNA cleavage reagents based on oxoruthenium(IV) complexes.[10-15] These complexes present a number of new approaches for understanding the mechanisms of DNA cleavage by metal complexes. These systems provide sensitive control over the redox potential of the cleavage agent, and we have recently shown that less reactive complexes show enhanced selectivity.[15] In addition, kinetic studies are possible using electrochemistry and optical spectroscopy.[11,14] The kinetics of the reaction of calf thymus DNA with $Ru(tpy)(L)O^{2+}$ (L = bpy, phen, and dppz) have been studied previously and can be explained using the model shown in Scheme 1.[14] The kinetic studies of the three complexes demonstrate that dissociation of the oxidized form is slow compared to reduction, i.e. $k_{off} \ll k_{cleavage} + k_X$. Meyer and co-workers have shown that related complexes undergo self-reduction in aqueous solution.[16]

An important aspect of these studies is that the kinetics determined by optical spectroscopy only give the kinetics for the reduction of the metal complex, not for cleavage of the DNA. In the terms of Scheme 1, the measurement gives $k_X + k_{cleavage}$, but not the relative rates of cleavage versus nonproductive reduction of the metal complex. However, since the reactions are stoichiometric, we can determine the precise yield of cleavage based on the metal complex. In our studies of oxoruthenium(IV), we have shown that the yield of sugar cleavage as determined by base release is 10%;[15] thus, $k_{cleavage}$ for sugar oxidation and k_X are competitive. Since our kinetic studies show that $k_{off} \ll k_X + k_{cleavage}$, the fastest process is apparently k_X, an idea we will explore in detail here. This result is similar to the recent isotope effect studies on FeBLM that show that $k_{cleavage} \ll k_X + k_{off}$.[9]

We report here on further mechanistic studies on DNA cleavage by $Ru^{IV}(tpy)(bpy)O^{2+}$ and $Ru^{III}(tpy)(bpy)OH^{2+}$ and on new investigations of the complex $Os^{IV}(tpy)(bpy)O^{2+}$, which is structurally similar to but considerably less reactive than the ruthenium analogue. Because of its lower reactivity, the relative rates of k_X and $k_{cleavage}$ for $Os(tpy)(bpy)O^{2+}$ are such that DNA oxidation does not occur, i.e. $k_{cleavage}$ cannot compete with k_X. However, DNA catalyzes the self-inactivation of the complex, and this catalysis is sequence-specific. In addition, we have also observed that the $Ru(tpy)(bpy)O^{2+}$ complex cleaves DNA both by guanine oxidation and by sugar oxidation at the C-1′ position.

Experimental Section

Metal Complexes. The complexes $[Ru(tpy)(bpy)OH_2](ClO_4)_2$ and $[Os(tpy)(bpy)OH_2](CF_3CO_2)_2$ were prepared according to published procedures.[17] The oxidized metal complexes were prepared by electrochemical oxidation of the corresponding $M(tpy)(bpy)OH_2^{2+}$ complexes in 10 mM phosphate buffer (pH 7.1), as described previously.[14] The applied potential was 0.8 V for $Ru(tpy)(bpy)O^{2+}$, 0.5 V for $Ru(tpy)(bpy)OH^{2+}$, and 0.6 V for $Os(tpy)(bpy)O^{2+}$. Electrolysis was continued until the current reached less than 5% of the initial value. For the ruthenium complexes, the results were not changed by using electrochemical oxidation compared to thermal oxidation using isolated complexes.

X-ray Crystallography. Crystals were grown by slow evaporation of an aqueous solution of $[Os(tpy)(bpy)OH_2](CF_3SO_3)_2$. X-ray data were collected on a Siemens P3/F 4-circle diffractometer in the Department of Chemistry at North Carolina State University. The cell constants were obtained from 16 reflections with 2Θ values between 12 and 22°. The structure was solved by Patterson and difference Fourier techniques and refined by blocked-cascade least-squares methods using SHELXTL. Hydrogen atoms were placed in calculated positions.

DNA Experiments. All DNA concentrations for polymeric DNA are given in terms of nucleotide phosphate. The concentrations of polymeric DNA obtained from Sigma and purified by standard procedures were determined using the following extinction coefficients: calf thymus DNA, ϵ(260 nm) = 6600 M^{-1} cm^{-1}; poly(dA)•poly(dT), ϵ(260 nm) = 6000 M^{-1} cm^{-1}; poly(dG)•poly(dC), ϵ(260 nm) = 7400 M^{-1} cm^{-1}. The quantity R corresponds to the ratio of [DNA-phosphate]/[metal complex]. Concentrations of DNA for oligomers in Figures 2 and 3 are in terms of actual concentration of oligomers determined by standard calculations based on oligomer composition.[18]

Solutions of the metal complex and the plasmid ϕX174 DNA solutions were diluted with bromophenol blue loading buffer and loaded onto 1% agarose gels containing ethidium bromide and electrophoresed for approximately 1 h at 44 V. The gels were photographed under UV light.

The synthetic oligonucleotides were acquired from the Oligonucleotide Synthesis Center in the Department of Pathology at UNC. Further purification was performed using FPLC with a MonoQ HR 5/5 column (Pharmacia) with a 30–45% gradient (Buffer A, 0.015 M NaOH; Buffer B, 0.015 M NaOH and 1.5 M NaCl). The collected solution was dialyzed (1000 molecular weight cutoff) against MilliQ water for 48 h and lyophylized to dryness. The oligonucleotide was resuspended in buffer, and its concentration was determined from the absorbance at 260 nm, as previously described.

(10) Grover, N.; Gupta, N.; Singh, P.; Thorp, H. H. *Inorg. Chem.* **1992**, *31*, 2014.
(11) Grover, N.; Thorp, H. H. *J. Am. Chem. Soc.* **1991**, *113*, 7030.
(12) Gupta, N.; Grover, N.; Neyhart, G. A.; Liang, W.; Singh, P.; Thorp, H. H. *Angew. Chem., Int. Ed. Engl.* **1992**, *31*, 1048.
(13) Gupta, N.; Grover, N.; Neyhart, G. A.; Singh, P.; Thorp, H. H. *Inorg. Chem.* **1993**, *32*, 310.
(14) Neyhart, G. A.; Grover, N.; Smith, S. R.; Kalsbeck, W. A.; Fairley, T. A.; Cory, M.; Thorp, H. H. *J. Am. Chem. Soc.* **1993**, *115*, 4423.
(15) Welch, T. W.; Neyhart, G. A.; Goll, J. G.; Ciftan, S. A.; Thorp, H. H. *J. Am. Chem. Soc.* **1993**, *115*, 9311–9312.
(16) Roecker, L.; Kutner, W.; Gilbert, J. A.; Simmons, M.; Murray, R. W.; Meyer, T. J. *Inorg. Chem.* **1985**, *24*, 3784–3791.
(17) Takeuchi, K. J.; Thompson, M. S.; Pipes, D. W.; Meyer, T. J. *Inorg. Chem.* **1984**, *23*, 1845.
(18) Fasman, G. D. *CRC Handbook of Biochemistry and Molecular Biology*; CRC Press: Boca Raton, FL, 1975; Vol. 1.

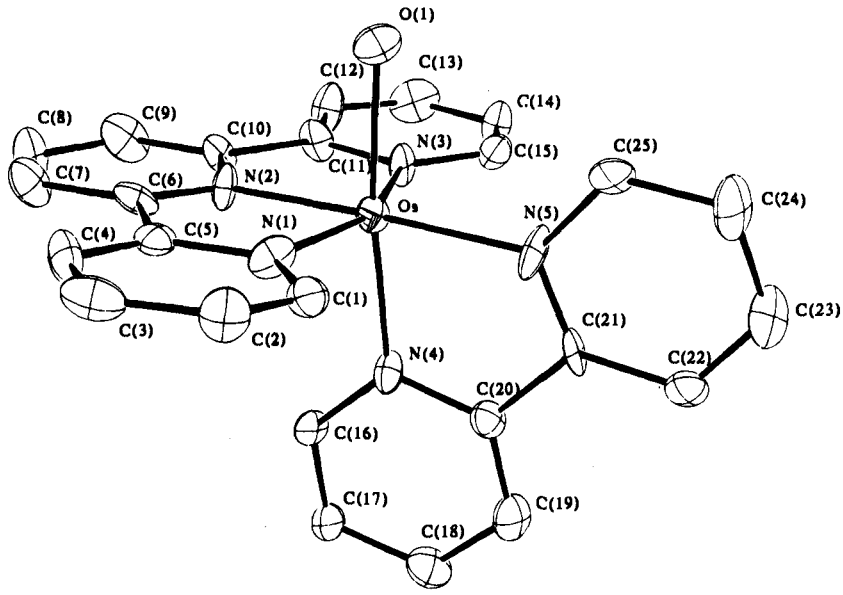

Figure 1. ORTEP diagram of the cation in $[Os(tpy)(bpy)OH_2](CF_3SO_2)_2$. Hydrogen atoms are omitted for clarity.

The 5′-end-^{32}P-labeled oligomer was prepared by using T4 polynucleotide kinase and deoxyadenosine 5′-[γ-^{32}P]-triphosphate (Amersham). The isolation of ^{32}P-labeled DNA was achieved by filtration with Centricon-10 (Amicon) at 0−5 °C for 45 min using ultracentrifugation, followed by an additional centrifugation in deionized water (1 mL) for 35 min. The extent of labeling was determined using a scintillation counter. The 3′-end-labeled oligomer was prepared in a similar fashion, except the labeling procedure involved terminal deoxynucleotidyl transferase (Gibco BRL) and 2′-dideoxyadenosine 5′-[α-^{32}P] triphosphate (Amersham), as described.[19]

For the self-complementary oligomer, the duplex was annealed by heating the DNA solution containing d(CGCAAATTTGCG) (90 μM), 0.1 M sodium phosphate buffer, and ^{32}P-end-labeled DNA at 90 °C for 8 min. This DNA solution was slowly cooled to room temperature for 6−8 h. The formation of the duplex was confirmed by using 20% non-denaturing polyacrylamide (acrylamide−bisacrylamide 19:1) gel electrophoresis at 4 °C, as described elsewhere.[19]

In cleavage reactions, the solution of the oxidized metal complex was immediately transferred into a phosphate buffer solution containing 4.0 μM of the synthetic DNA and ~3 nCi of the 5′- or 3′-end-^{32}P-labeled oligomer. The reaction mixture was maintained at room temperature for the desired period, quenched with either 95% EtOH (10 μL) or sodium ascorbate (10 mM), and lyophilized to dryness. The samples that were subjected to base treatment were resuspended in 0.7 M piperidine (60 μL) and maintained at 90 °C for 30 min. Prior to analysis, the reaction mixtures were lyophilized, treated with water (20 μL), lyophilized, and resuspended in the gel-loading buffer (5 μL) containing 80% formamide, 0.25% bromophenol blue, and 0.25% xylene cyanol FF.

The DNA fragments were analyzed using 20% polyacrylamide (acrylamide−bisacrylamide = 19:1) gel electrophoresis under denaturing conditions (7 M urea). The electrophoresis was performed at a potential of 300 V for 60 min and raised to 1500 V for 140 min. Cleavages were visualized using Kodak X-Omat Ar-5 film at −78 °C for 18−24 h. Quantitation of the extent of cleavage was performed by integration of the optical density as a function of the band area using an Apple OneScanner and the Image program from the NIH.

Product Analysis for 5-MF. Calf thymus DNA (ctDNA) (Sigma) was purified sequentially by phenol, phenol−chloroform extraction (twice), and ethanol precipitation, as described elsewhere.[19] A solution of $Ru(tpy)(bpy)O^{2+}$ (1.2 mg) in 10 mM sodium phosphate buffer (150 μL, pH 7.06) was added to a solution containing ctDNA (2.5 mg) dissolved in 10 mM sodium phosphate buffer. The resulting solution was maintained at room temperature for 50 min and quenched by adding 95% ethanol (1 mL). After vortexing, the solution was cooled to −20 °C for 30 min and centrifuged at 4 °C for 6 min (12 400 rpm). The resulting wet brown pellet was gently washed with 95% ethanol and centrifuged at 4 °C. This procedure was repeated, and the pellet was then lyophilized to dryness and stored at −20 °C.

The following procedures were carried out in the dark to avoid the photopolymerization of the furanone product. The lyophilized pellet was dissolved in 200 μL of water and transferred to a polytetrafluoroethylene-capped borosilicate vial (0.3 mL capacity) and heated at 90 °C for 30 min. The solution was cooled to −20 °C for 6 h to condense any volatile organics liberated during heating. After defrosting, the solution was extracted with chloroform (100 μL × 2) at room temperature. The combined organic fractions were concentrated by slowly evaporating the solvent at 4 °C until the volume of the solution was 5−10 μL. The resulting solution was sealed and stored in the dark at −20 °C prior to analysis. HPLC analysis was performed using a Millenium 2010 HPLC (Millipore, Inc.) with a Photodiode Array Detector (Waters 996). Separation of 5-MF was acheived using a Rainin Microsorb-MV C-18 column (3 μM, 4.6 × 100 mM) eluted with water and a 0−20% acetonitrile gradient at a flow rate of 1 mL/min. GC-MS analysis was performed using a Hewlett Packard 5890 gas chromatograph fitted with a HP 5971 mass selective detector. The injection temperature was 250 °C and the detection temperature was 280 °C. The oven temperature was held at 35 °C for 2 min, and the temperature was increased by 10 °C/min for 30 min. The 5-MF product was detected at 4.1 min with a molecular weight of 96. The GC-MS data are given in the supplementary material.

Kinetic Measurements. Solutions of calf thymus DNA, poly(dG)•poly(dC), and poly(dA)•poly(dT) were prepared using 50 mM phosphate buffer and were checked by UV−vis spectroscopy before use. $[Os(tpy)(bpy)O](CF_3SO_3)_2$ was prepared by electrochemical oxidation at 0.6 V of the corresponding aqua complex in 50 mM phosphate buffer and used immediately. Kinetic data were obtained on an OLIS modified Cary 14 UV−vis spectrometer. Rate constants were obtained by plotting $\ln[A_\infty - A_t]$ versus time.

Results

Synthesis and Structure. The $Os(tpy)(bpy)OH_2^{2+}$ complex is readily synthesized by the methods reported by Meyer et al.[17] Single crystals of $[Os(tpy)(bpy)OH_2](CF_3SO_2)_2$ suitable for X-ray diffraction were grown by slow evaporation of an aqueous solution. The crystal structure is useful for our studies because we are interested in altering the reactivity by changing the metal center without changing the structure of the metal complex. The X-ray crystal structure of the $Os(tpy)(bpy)OH_2^{2+}$ cation is shown in Figure 1. The crystal data are given in Table 1, the fractional

(19) Maniatis, T.; Fritsch, E. F.; Sambrook, J. *Molecular Cloning: A Laboratory Manual*, 2nd ed.; Cold Spring Harbor Press: Cold Spring Harbor, NY, 1989.

Table 1. Crystal Data for $[Os(tpy)(bpy)OH_2](CF_3SO_3)_2$

formula	$C_{27}H_{21}N_5O_7F_6S_2Os$
mol wt, g/mol	895.82
crystal size, mm	0.47 × 0.25 × 0.15
λ(Mo Kα), Å	0.71073
a, Å	11.803(8)
b, Å	15.773(9)
c, Å	17.132(11)
β, deg	106.17(4)
V, Å^3	3063(3)
space group	$P2_1/a$
Z	4
D_{calc}, g/cm^3	1.94
μ(Mo Kα), cm^{-1}	43.9
F(000), e$^-$	1744
no. of reflecns measd	3270
R_{int}	0.033
function minimized	$\Sigma w(\|F_o\| - \|F_c\|)^2$
least-squares weights	$1/[\sigma^2(F) + 0.001F^2]$
no of observns, $I \geq 2\sigma(I)$	2674
$R = \Sigma\|\|F_o\| - \|F_c\|\|/\|F_o\|$	0.069
$R_w = [\Sigma w(\|F_o\| - \|F_c\|)^2/\Sigma wF_o^2]^{1/2}$	0.091
goodnes of fit, S	1.1

coordinates in Table 2, and selected bond lengths and angles in Table 3.

The structure of $Os(tpy)(bpy)OH_2^{2+}$ is best described as a distorted octahedron. The relatively long Os−OH_2 bond length of 2.13 Å shows that there is no multiple bonding between osmium and oxygen, as expected for this reduced species. Coordination of the tpy ligand is typical for tpy coordinated to osmium or ruthenium with a significantly shorter bond to the middle pyridyl ring compared to the outer rings. Related complexes include $Ru(tpy)(bpy)OH_2^{2+}$ and $[Os(tpy)(bpy)]_2O^{4+}$, which have been previously characterized by X-ray diffraction.[20,21] A comparison of relevant bond lengths and bond angles for $Os(tpy)(bpy)OH_2^{2+}$ and $Ru(tpy)(bpy)OH_2^{2+}$ is given in Table 3. The data in Table 3 clearly show that the osmium and ruthenium complexes have nearly identical structures.

Oxidation of $M(tpy)(bpy)OH_2^{2+}$ at neutral pH occurs via two one-electron, one-proton steps:[22]

$$Ru(tpy)(bpy)OH_2^{2+} \rightarrow Ru(tpy)(bpy)OH^{2+} + H^+ + e^- \quad (2)$$

$$Ru(tpy)(bpy)OH^{2+} \rightarrow Ru(tpy)(bpy)O^{2+} + H^+ + e^- \quad (3)$$

Thus, the oxidized forms are stabilized by deprotonation of the aqua and hydroxo ligands. As a result, the metal−nitrogen bonds to the polypyridyl ligands are not required to contract to stabilize the higher oxidation state. A striking example of this phenomenon can be seen by comparing the bond lengths in $Ru(tpy)(bpy)OH_2^{2+}$ or $Ru(tpy)(tmen)OH_2^{2+}$ to those in the dioxoruthenium(VI) complex $Ru(tpy)(OH_2)(O)_2^{2+}$.[23] Even though the dioxo complex is oxidized by four electrons relative to the aqua complexes, the bond lengths to tpy are identical within experimental error, as we have pointed out previously.[10] Thus, the stabilization of the higher oxidation state is accomplished solely by the mutliple bonding interactions to the oxo ligands. As a result, we may consider the structures of all of the redox congeners ($M^{II}OH_2^{2+}$, $M^{III}OH^{2+}$, and $M^{IV}O^{2+}$) of $M(tpy)(bpy)OH_2^{2+}$ to be very similar with regard to the M(tpy)(bpy) fragment. Since all of the redox states have the same charge, the only difference in the structures is the number of protons on the oxygen ligand and variation in the metal−oxygen bond length.

Table 2. Atomic Coordinates (×10^4) and Isotropic Thermal Parameters (Å^2 × 10^3) for $[Os(tpy)(bpy)OH_2](CF_3SO_3)_2$

	x	y	z	U^a
Os	1332(1)	5364(1)	7881(1)	30(1)
N(1)	−356(11)	5075(8)	7144(8)	39(5)
N(2)	603(9)	6484(7)	7644(7)	30(4)
N(3)	2696(10)	6103(7)	8526(7)	33(4)
N(4)	2079(10)	5267(7)	6959(7)	33(5)
N(5)	2142(10)	4217(7)	8082(8)	43(5)
O(1)	605(9)	5275(7)	8886(7)	51(5)
C(1)	−818(14)	4302(10)	6918(9)	39(6)
C(2)	−1964(13)	4178(11)	6515(9)	46(6)
C(3)	−2699(15)	4868(12)	6260(9)	50(7)
C(4)	−2233(13)	5661(12)	6477(9)	47(6)
C(5)	−1055(13)	5770(10)	6917(8)	37(6)
C(6)	−480(12)	6569(9)	7215(8)	32(5)
C(7)	−996(15)	7387(10)	7019(10)	49(7)
C(8)	−333(15)	8082(10)	7291(11)	52(7)
C(9)	808(17)	7979(11)	7814(11)	58(8)
C(10)	1289(13)	7175(9)	7977(8)	37(6)
C(11)	2459(12)	6968(10)	8491(9)	37(6)
C(12)	3276(14)	7528(11)	8919(12)	57(8)
C(13)	4358(15)	7269(12)	9372(11)	63(8)
C(14)	4613(13)	6414(10)	9407(10)	45(6)
C(15)	3772(13)	5835(10)	9013(9)	42(6)
C(16)	1979(13)	5846(8)	6361(8)	34(6)
C(17)	2578(13)	5794(11)	5794(9)	42(6)
C(18)	3342(15)	5099(12)	5823(10)	50(7)
C(19)	3450(14)	4485(10)	6412(10)	45(7)
C(20)	2799(13)	4600(9)	6960(9)	35(6)
C(21)	2809(11)	3968(8)	7615(8)	30(5)
C(22)	3430(13)	3207(10)	7700(9)	41(6)
C(23)	3405(14)	2677(10)	8325(12)	51(7)
C(24)	2725(16)	2894(10)	8831(12)	61(7)
C(25)	2099(15)	3661(10)	8710(9)	43(6)
C(26)	1382(15)	630(11)	8435(10)	53(7)
F(1)	693(10)	56(8)	7967(7)	85(5)
F(2)	1630(12)	1182(7)	7939(7)	97(6)
F(3)	726(12)	1009(10)	8829(8)	123(7)
S(1)	2654(4)	157(3)	9117(3)	44(2)
O(2)	3241(11)	−221(10)	8586(8)	79(6)
O(3)	2188(12)	−437(7)	9550(8)	71(6)
O(4)	3251(11)	850(7)	9591(6)	65(5)
C(27)	745(14)	2979(11)	5362(10)	51(7)
F(4)	1373(12)	2919(10)	4829(9)	118(7)
F(5)	345(10)	3760(6)	5311(9)	96(6)
F(6)	1498(10)	2911(9)	6089(7)	97(6)
S(2)	−406(4)	2199(3)	5197(3)	48(2)
O(5)	210(12)	1401(7)	5285(8)	72(6)
O(6)	−1118(11)	2396(7)	4407(8)	77(6)
O(7)	−931(13)	2405(9)	5834(10)	88(7)

[a] *Equivalent isotropic U defined as one-third of the trace of the orthogonalised U_{ij} tensor.

DNA Binding. Since the $Os(tpy)(bpy)OH_2^{2+}$ complex is isostructural with $Ru(tpy)(bpy)OH_2^{2+}$, it should have the same DNA binding constant. We have reported recently the details of a method for determining binding constants that relies on the different abilities of free and bound metal complexes to quench the intense emission of the $Pt_2(pop)_4^{4-}$ excited state by electron or energy transfer (pop = $P_2O_5H_2^{2-}$).[24] We have measured the binding constant for both $Ru(tpy)(bpy)OH_2^{2+}$ and $Os(tpy)(bpy)OH_2^{2+}$ using this method. The fitted binding constants of K_b(Os) = 550 ± 160 M^{-1} and K_b(Ru) = 660 ± 200 M^{-1} are identical within experimental error.[24]

The binding constants of the oxidized forms cannot be determined because addition of DNA to the oxidized complexes

(20) Roecker, L. E. Thesis, University of North Carolina at Chapel Hill, 1985.
(21) Seok, W. K. Thesis, University of North Carolina at Chapel Hill, 1988.
(22) Meyer, T. J. *J. Electrochem. Soc.* **1984**, *131*, 221C.
(23) Dovletoglou, A.; Adeyemi, S. A.; Lynn, M. H.; Hodgson, D. J.; Meyer, T. J. *J. Am. Chem. Soc.* **1990**, *112*, 8989−8990.
(24) Kalsbeck, W. A.; Thorp, H. H. *J. Am. Chem. Soc.* **1993**, *115*, 7146−7151.

Table 3. Selected Bond Distances and Bond Angles for $Ru(tpy)(bpy)OH_2^{2+}$ and $Os(tpy)(bpy)OH_2^{2+}$

	$Os-OH_2$	$Ru-OH_2$[a]
	Selected Distances (Å)	
$M-O_w$	2.130(14)	2.136(5)
$M-N_1$	2.101(12)	2.053(6)
$M-N_2$	1.956(11)	1.960(6)
$M-N_3$	2.051(11)	2.062(7)
$M-N_4$	2.023(15)	2.0156)
$M-N_5$	2.033(12)	2.068(6)
	Selected Angles (deg)	
$O-M-N_1$	86.6(5)	88.5(2)
$O-M-N_2$	88.6(5)	86.9(2)
$O-M-N_3$	92.1(5)	87.4(2)
$O-M-N_4$	171.6(4)	174.9(3)
$O-M-N_5$	94.6(5)	96.9(5)
N_1-M-N_2	77.5(5)	79.8(2)
N_1-M-N_3	157.7(5)	158.7(3)
N_1-M-N_4	93.7(5)	93.2(2)
N_1-M-N_5	103.3(5)	99.3(2)
N_2-M-N_3	80.3(4)	79.1(3)
N_2-M-N_4	99.7(5)	98.1(3)
N_2-M-N_5	176.7(6)	176.1(3)
N_3-M-N_4	92.1(5)	92.7(2)
N_3-M-N_5	99.0(4)	102.0(3)
N_4-M-N_5	77.1(6)	78.1(3)

[a] Taken from ref 21.

causes immediate reduction of the complexes. However, we may consider the reduced $M(tpy)(bpy)OH_2^{2+}$ forms as nearly identical structurally, based on the considerations enumerated above. The only caveat required is that the reduced forms contain OH_2 or OH ligands that could potentially hydrogen bond to DNA phosphates, whereas the $M^{IV}O^{2+}$ form has no hydrogen bond donor. Thus, the affinities of the reduced forms may be somewhat higher than the oxo form; however, based on recent estimates for metal−aqua binding affinities, the affinity of the reduced forms can be no more than 1−1.5 kcal/mol greater than that of the $M^{IV}O^{2+}$ form.[25,26]

DNA Oxidation. (a) $Ru(tpy)(bpy)O^{2+}$−Sugar Oxidation. The 5′-end labeled oligonucleotide d(5′-$A_1T_2A_3C_4G_5C_6A_7A_8G_9G_{10}G_{11}C_{12}A_{13}T_{14}$-3′) was subjected to oxidation by electrogenerated $Ru(tpy)(bpy)O^{2+}$ for 3 min. This oligonucleotide was selected because it has been shown to exhibit only a random-coil structure in solution,[27] and we wanted to maximize the probability of reaction with the metal complex. We therefore prevented as much as possible structural complexity from interfering with the intrinsic reactivity of various sites on the oligomer toward the cleavage agent. As shown in Figure 2, there is some frank scission, especially at C_6, A_7, and C_{12}, that is apparent prior to piperidine treatment. These sites must arise from sugar oxidation, because isolated cytosine and adenine are not reactive toward oxidation by $Ru(tpy)(bpy)O^{2+}$[28] and because base oxidations usually produce only piperidine-labile cleavages.[27,29] The product bands are indicative of 1′-oxidation, as observed with Cu-phen (Scheme 2).[30] The lesion at A_7 migrates between the phosphate-terminated bands and migrates with the phosphate-terminated bands following piperidine treatment. This terminus must be a derivatized phosphate (**3**) that is hydrolyzed to an authentic phosphate (3′-**2**) upon piperidine treatment.

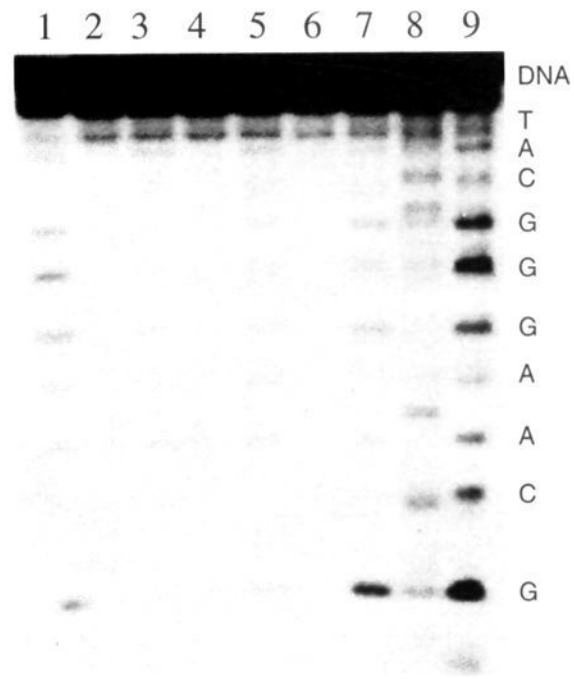

Figure 2. Autoradiogram of a polyacrylamide gel showing the results of the oxidation of 5′-^{32}P-labeled random coil oligomer d(5′-ATACGCAAGGGCAT-3′) (4.0 μM) by $Ru^{IV}O^{2+}$, $Ru^{III}OH^{2+}$, and $Os^{IV}O^{2+}$ (all metal concentrations 24 μM). Lane 1, Maxam−Gilbert G + A reaction; lane 2, untreated DNA; lane 3, DNA + piperidine (90 °C, 30 min); lane 4, DNA treated with $Os(tpy)(bpy)O^{2+}$ (60 min); lane 5, lane 4 + piperidine; lane 6, $Ru(tpy)(bpy)OH^{2+}$ (60 min); lane 7, lane 6 + piperidine; lane 8, $Ru(tpy)(bpy)O^{2+}$ (3 min); lane 9, lane 8 + piperidine. Concentrations and other conditions are given in the Experimental Section.

Following piperidine treatment, a much larger number of DNA lesions are apparent. These include an increase in cleavage at C_6 as well as new bands at A_8 and A_{13} that must arise from piperidine-labile lesions produced by sugar oxidation. This observation is also suggestive of 1′ oxidation, which generates a ribonolactone residue (**1**) that often requires base treatment to induce strand scission but does give immediate base release.[30−32] Quantitation of the extent of cleavage at A, T, and C with and without piperidine treatment shows that the yield of frank scission is about one-third of that realized following piperidine treatment. Also consistent with 1′ chemistry is the observation that depletion of oxygen from the cleavage reaction solution does not alter the results (gel shown in the supplementary material).

The results of oxidation of the self-complementary oligomer d(5′-$C_1G_2C_3A_4A_5A_6T_7T_8T_9G_{10}C_{11}G_{12}$-3′) are shown in Figure 3A. As in the single-stranded oligomer, a modified phosphate terminus is apparent prior to piperidine treatment at A_5 in the 5′-labeled fragment, indicating that the chemical mechanism is the same in double- and single-stranded oligomers. According to the mechanism shown in Scheme 2, 5′-phosphate termini (5′-**2**) should be generated on the 3′-labeled fragment, regardless of whether a modified terminus is produced on the 5′-labeled fragment. Shown in Figure 3B are the results of oxidizing the double-stranded oligomer labeled on the 3′ end. Only 5′-phosphate-terminated bands are observed, even when modified termini are formed in the 5′-labeled fragment. Labeling the 3′-end of the single-stranded oligomer shown in Figure 2 also gives only 5′-phosphate termini (data not shown).

Since we have previously reported the production of free bases,[14,15] the remaining undetected product in Scheme 2 is the furanone 5-methylene-2(5*H*)-furanone (5-MF, **4**) derived from the sugar ring. Extraction of the reaction mixture with chloroform by a procedure similar to that of Sigman and co-

(25) Kalsbeck, W. A.; Thorp, H. H. *Inorg. Chem.* **1994**, *33*, 3427−3429.
(26) Black, C. B.; Cowan, J. A. *J. Am. Chem. Soc.* **1994**, *116*, 1174−1178.
(27) Chen, X.; Burrows, C. J.; Rokita, S. E. *J. Am. Chem. Soc.* **1992**, *114*, 322.
(28) Neyhart, G. A.; Cheng, C.-C.; Thorp, H. H. *J. Am. Chem. Soc.* **1995**, *117*, 1463−1471.
(29) Chen, X.; Burrows, C. J.; Rokita, S. E. *J. Am. Chem. Soc.* **1991**, *113*, 5884.
(30) Sigman, D. S. *Acc. Chem. Res.* **1986**, *19*, 180.
(31) Sugiyama, H.; Tsutsumi, Y.; Fujimoto, K.; Saito, I. *J. Am. Chem. Soc.* **1993**, *115*, 4443−4448.
(32) Duff, R. J.; de Vroom, E.; Geluk, A.; Hecht, S. M.; van der Marel, G. A.; van Boom, J. H. *J. Am. Chem. Soc.* **1993**, *115*, 3350.

Scheme 2

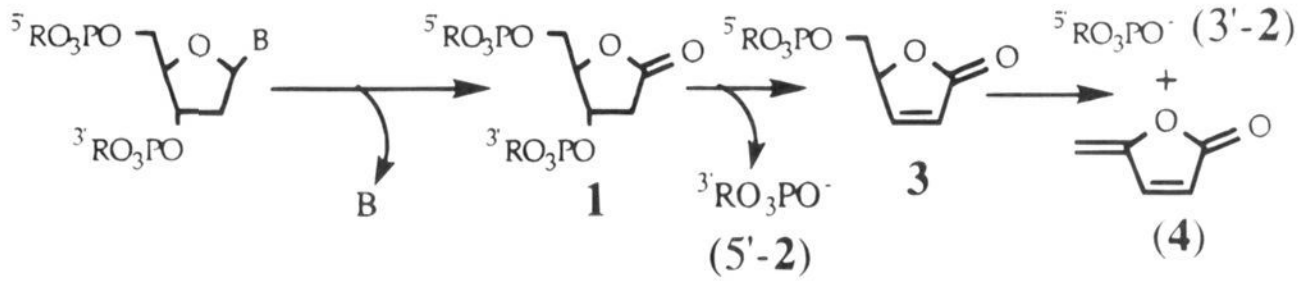

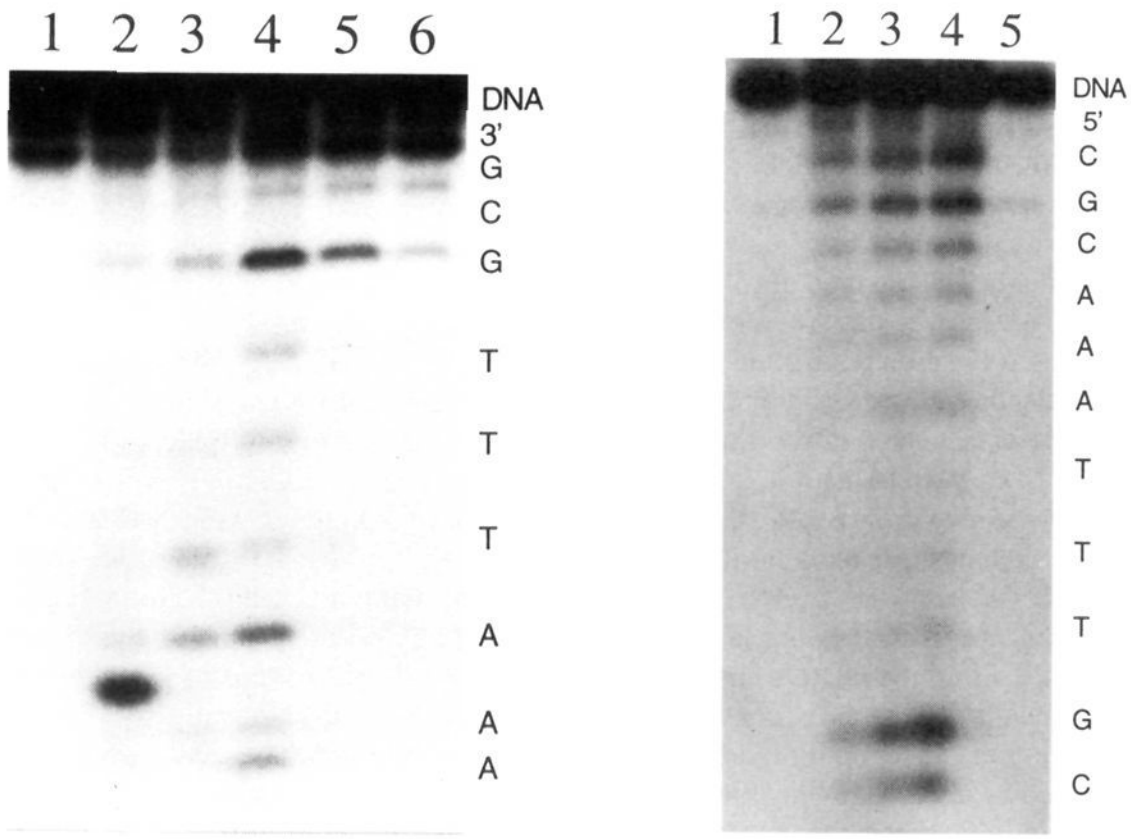

Figure 3. Autoradiogram of a polyacrylamide gel showing the results of oxidation of the (A) 5′- and (B) 3′-end-^{32}P-labeled self-complementary duplex d(5′-CGCAAATTTGCG-3′) (4.0 μM) with Ru(tpy)(bpy)O^{2+} (24 μM). (A, left) Lane 1, 5′-labeled DNA + distamycin + piperidine; lane 2, treatment with Ru(tpy)(bpy)O^{2+} only; lane 3, Ru(tpy)(bpy)O^{2+} + heat treatment; lane 4, Ru(tpy)(bpy)O^{2+} + piperidine treatment; lane 5, distamycin + Ru(tpy)(bpy)O^{2+} + piperidine; lane 6, Maxam−Gilbert G reaction. (B, right) Lane 1, 3′-end-labeled DNA + distamycin + piperidine; lane 2, Ru(tpy)(bpy)O^{2+} treatment only; lane 3, Ru(tpy)(bpy)O^{2+} + heat treatment; lane 4, Ru(tpy)(bpy)O^{2+} + piperidine; lane 5, distamycin + Ru(tpy)-(bpy)O^{2+} + piperidine. Concentrations and other conditions are given in the Experimental Section.

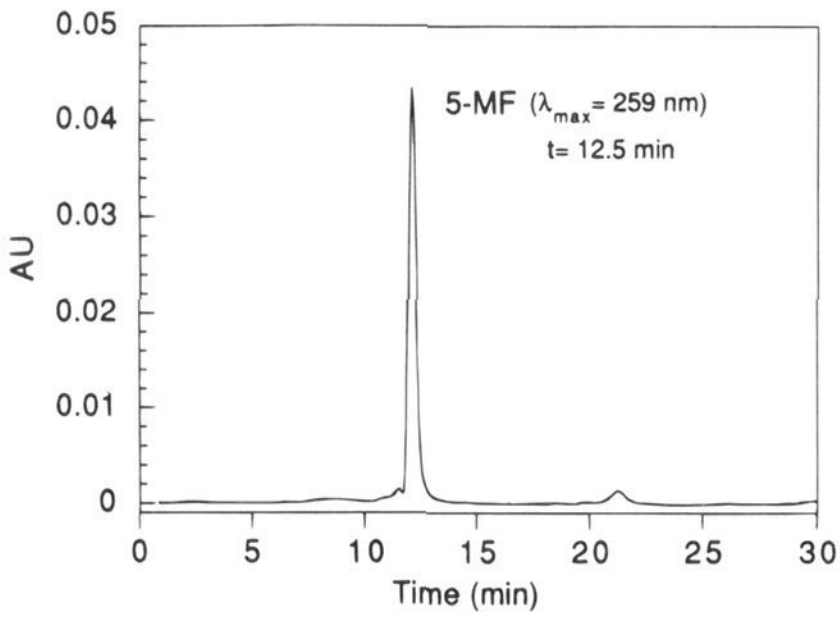

Figure 4. HPLC of a chloroform extract of the reaction of Ru(tpy)-(bpy)O^{2+} with calf thymus DNA in pH 7 phosphate buffer. The peak due to 5-MF (12.5 min) gave an absorbance maximum at 259 nm, which was determined using diode array detection. Identical retention time and absorbance maximum were determined for an authentic sample. The small peak at 21 min is a product of the known photopolymerization reaction.

workers[33] produces a solution whose HPLC and GC-MS are consistent with the formation of **4**. Shown in Figure 4 is the HPLC obtained on the chloroform fraction, which shows a peak at 12.5 min. This peak has been identified as arising from **4** by comparison with the HPLC of an authentic sample prepared from angelikalactone by published procedures.[34] The furanone **4** was identified by both retention time and optical spectrum (λ_{max} = 259 nm) using a diode array detector. The GC-MS data for the chloroform extract are given in the supplementary material, and the authentic sample again has an identical retention time (4.1 min) and mass spectrum (MW 96) to the reaction product. It is therefore clear that the species in the chromatograms is **4** and not an isomeric furanone that can arise from 3′ oxidation.[35] We have therefore detected all of the expected products for 1′ sugar oxidation.

The observation of 1′ oxidation implicates binding and reaction of the complex in the minor groove.[30−33] In related cleavage reactions, inhibition of cleavage by distamycin and other groove binders has been used to support action of small molecules in the minor groove,[36] since distamycin is known to bind to the minor groove of duplex DNA. In fact, the crystal structure of distamycin bound to the double-stranded oligomer from Figure 3 has been determined[37,38] and shows binding of the drug to the central AAATTT segment. Oxidation of the

(33) Goyne, T. E.; Sigman, D. S. *J. Am. Chem. Soc.* **1987**, *109*, 2846.

(34) Grundmann, C.; Kober, E. *J. Am. Chem. Soc.* **1955**, *77*, 2332−2333.

(35) Sitlani, A.; Long, E. C.; Pyle, A. M.; Barton, J. K. *J. Am. Chem. Soc.* **1992**, *114*, 2303.

(36) Kuwabara, M.; Yoon, C.; Goyne, T.; Thederahn, T.; Sigman, D. S. *Biochemistry* **1986**, *25*, 7401−7408.

(37) Coll, M.; Frederick, C. A.; Wang, A. H.-J.; Rich, A. *Proc. Natl. Acad. Sci. U.S.A.* **1987**, *84*, 8385−8389.

(38) Kennard, O.; Hunter, W. N. *Angew. Chem., Int. Ed. Engl.* **1991**, *30*, 1254−1277.

duplex by Ru(tpy)(bpy)O^{2+} in the presence of distamycin leads to protection of the duplex from oxidation, as shown in Figure 3. Further, the protection occurs specifically in the AAATTT segment and not on the ends, in accordance with the known distamycin binding locus. This experiment further confirms binding and reaction of the complex in the minor groove and is consistent with the observation of 1′ oxidation.

(b) Ru(tpy)(bpy)O^{2+}−Guanine Oxidation. In addition to the sugar oxidations at A, T, and C, the guanine sites show enhanced cleavage upon piperidine treatment. This result is consistent with a second pathway involving oxidation of the guanine base, which is known to produce a piperidine-labile lesion.[27,29] We have observed direct oxidation of both free guanine and guanine incorporated in mononucleotides.[28] The extent of cleavage at guanine is considerably greater than that observed at the other sites. Some of the cleavage at guanine may arise from sugar oxidation; indeed, oxidation of calf thymus DNA by Ru(tpy)(bpy)O^{2+} does lead to the release of free guanine,[14] which must arise from oxidation of guanine sugars.[39] Nonetheless, the amount of guanine released is similar to that of the other bases, which suggests that most of the cleavage at G apparent in Figure 2 arises from base oxidation.

It therefore appears that DNA oxidation by Ru(tpy)(bpy)-O^{2+} proceeds via two mechanisms: a sugar oxidation pathway involving 1′ oxidation that produces frank and base-labile scissions and another base oxidation pathway that leads only to base-labile lesions at guanine. From the relative amounts of cleavage, it appears that the guanine pathway is considerably more efficient. In fact, quantitation of the yield of cleavage at each site by densitometry shows that following piperidine treatment, the yield of cleavage is about 7 times larger at G than at A, T, and C on a per nucleotide basis. This observation is consistent with related studies on monomeric nucleotide oxidations that show that guanine nucleotide oxidation is faster than oxidation of nucleotides of A, T, and C.[28]

(c) Ru(tpy)(bpy)OH^{2+}. The complex Ru(tpy)(bpy)OH^{2+} is a weaker oxidant than Ru(tpy)(bpy)O^{2+} by 120 mV and is primarily only a one-electron oxidant, since the only accessible couple is the (III/II) reduction. In contrast, Ru(tpy)(bpy)O^{2+} can act as both a one- or two-electron oxidant, as discussed below. The $Ru^{III}OH^{2+}$ complex can access two-electron pathways via unfavorable disproportionation to $Ru^{IV}O^{2+}$ and $Ru^{II}OH_2^{2+}$,[40] and it is likely that any reactivity toward DNA is observed from $Ru^{IV}O^{2+}$ generated via this mechanism. Since the $Ru^{III}OH^{2+}$ complex is isostructural with the $Ru^{IV}O^{2+}$ complex, we expected cleavage by $Ru^{III}OH^{2+}$, if any occurred at all, to be selective for the most thermodynamically favorable pathway. Treatment of calf thymus DNA with Ru(tpy)(bpy)-OH^{2+} does not produce any free bases that are detectable by HPLC, suggesting that sugar oxidation is too slow to compete with other reduction pathways. Accordingly, no frank scission is apparent upon oxidation of the 5′-labeled oligonucleotide by Ru(tpy)(bpy)OH^{2+} (Figure 2). However, piperidine treatment does show selective cleavage of the oligonucleotide at guanine, consistent with base oxidation. Thus, for the stronger oxidant Ru(tpy)(bpy)O^{2+}, sugar oxidation is fast enough to compete with base oxidation, but for Ru(tpy)(bpy)OH^{2+}, only base oxidation is observed. This result is consistent with the relative yields of base and sugar oxidation observed with Ru(tpy)(bpy)O^{2+} in indicating that base oxidation is more efficient than sugar oxidation.

(d) Os(tpy)(bpy)O^{2+}. The oxidized Os(tpy)(bpy)O^{2+} complex has not yet been isolated. To date, we have been able only to generate the oxidized complex in solution by controlled potential electrolysis of a solution of Os(tpy)(bpy)OH_2^{2+} at 0.6 V. The spectra of the oxidized and reduced complexes synthesized in our laboratory agree well with those previously reported.[17] Addition of Os(tpy)(bpy)O^{2+} generated by controlled potential electrolysis to plasmid DNA effects conversion of the supercoiled form I to the nicked circular form II (gel shown in the supplementary material).

The plasmid experiment is very sensitive to low cleavage activity, because isomerization from form I to form II requires only a single oxidation event in the entire plasmid, and supercoiled DNA contains many strained structures that might be considerably more reactive than simple single- and double-stranded regions.[41] Shown in Figure 2 are the results of treatment of the single-stranded oligonucleotide with Os(tpy)-(bpy)O^{2+}. As seen in lane 4, there is no detectable strand scission immediately following treatment. After treatment with piperidine, still no significant cleavage is observed above the background. The Ru(tpy)(bpy)O^{2+} reactions were run for only 3 min while the Os(tpy)(bpy)O^{2+} reactions were run for 1 h. We have reported previously that treatment of calf thymus DNA with Os(tpy)(bpy)O^{2+} does not lead to base release.[15] This result, combined with those in Figure 2, shows that Os(tpy)-(bpy)O^{2+} is not capable of oxidizing DNA by either sugar or base oxidation except in supercoiled plasmids. The reduced forms do bind covalently to DNA via replacement of aqua ligands by DNA bases,[42−44] which could provide a mechanism for plasmid isomerization.

When Os(tpy)(bpy)O^{2+} is treated with calf thymus DNA, the reduction of the metal complex from Os(IV) to Os(III) is apparent from the absorbance spectra, in agreement with previous reports.[17] This is in contrast to Ru(tpy)(bpy)O^{2+}, where the final product of DNA oxidations is Ru(tpy)(bpy)-OH_2^{2+}.[11] The resulting Os(III) complex can be converted to Os(II) by treating the solution at the end of a kinetic run with excess sodium hydrosulfite. Treatment with this reducing agent produces Os(tpy)(bpy)OH_2^{2+}, as indicated by the absorption spectra.[17] The reactions of DNA with Os(tpy)(bpy)O^{2+} were run under conditions of at least a 10-fold DNA excess with DNA concentrations of 1.0 to 3.0 mM and an osmium concentration of 0.1 mM. First-order rate constants were obtained from plots of $\ln[A_\infty - A_t]$ versus time, which were linear over multiple half-lives. Table 4 shows the rate constants obtained with varying DNA concentrations. Unlike Ru(tpy)-(bpy)O^{2+}, which is stable for hours in buffered solution, the osmium analogue decomposes in the absence of DNA with a measurable rate constant of $k_{obs} = (1.0 \pm 0.2) \times 10^{-4}$ s^{-1}.

Table 4 also shows the results of the reaction run under pseudo-first-order conditions with a fixed DNA concentration of 3.0 mM and variable osmium complex concentrations of 0.01−0.3 mM. The variation in rate constant is not significant, which is consistent with the pseudo-first-order conditions imposed by the large excess of DNA.

The results in Table 4 show that DNA accelerates the reduction of Os(tpy)(bpy)O^{2+}; however, the results in Figure 2 show that DNA is not damaged in the process. The DNA must therefore be catalyzing the self-inactivation of the metal complex. The self-inactivation of complexes in this family has

(39) In fact, there is a weak band on the gel at G_{11} in the absence of piperidine (Figure 2, lane 8) that migrates behind the phosphate-terminated fragments and must correspond to a derivatized phosphate terminus generated from sugar oxidation at the guanosine site.

(40) Thompson, M. S.; Meyer, T. J. *J. Am. Chem. Soc.* **1982**, *104*, 4106.

(41) Palecek, E. *Crit. Rev. Biochem. Mol. Biol.* **1991**, *26*, 151−226.

(42) Grover, N.; Welch, T. W.; Fairley, T. A.; Cory, M.; Thorp, H. H. *Inorg. Chem.* **1994**, *33*, 3544−3548.

(43) Grover, N.; Gupta, N.; Thorp, H. H. *J. Am. Chem. Soc.* **1992**, *114*, 3390.

(44) Barton, J. K.; Lolis, E. *J. Am. Chem. Soc.* **1985**, *107*, 708.

Table 4. First-Order Rate Constants for Reduction of $Os(tpy)(bpy)O^{2+}$

[DNA] (mM)	[Os] (mM)	k_{obs} (10^3 s^{-1})[a]
0.0	0.10	0.10 ± 0.02
1.0	0.10	0.38 ± 0.05
1.5	0.10	0.68 ± 0.06
2.0	0.10	0.97 ± 0.21
2.5	0.10	1.23 ± 0.21
3.0	0.10	1.31 ± 0.21
3.0	0.30	1.44 ± 0.02
3.0	0.20	1.26 ± 0.13
3.0	0.15	1.29 ± 0.04
3.0	0.12	1.23 ± 0.31
3.0	0.03	1.16 ± 0.08
3.0	0.01	1.10 ± 0.23

[a] Determined from single-exponential kinetic traces using linear fits of plots of $\ln[A_\infty - A_t]$ versus time.

Table 5. Rate Enhancement for $Os(tpy)(bpy)O^{2+}$ Reduction in the Presence of Nucleic Acid Polymers

polymer	k_{cat}/k_{uncat}[a]
DNA	13.1 ± 1.4
poly(dA)·poly(dT)	44 ± 6
poly(dG)·poly(dC)	10.4 ± 0.6

[a] Measured at 0.1 mM $Os(tpy)(bpy)O^{2+}$ and 3.0 mM nucleic acid.

been investigated in detail and proceeds via the attack of one complex on the polypyridyl ligands of a second complex.[16,45,46] At basic pH, the rate of these reactions is limited by deprotonation of the polypyridyl ligand; however, at neutral pH, a complex dependence is observed where the rate increases with the concentration of the metal complex.[16,45,46] Nearly complete recovery of the reduced form of the complex is observed, because many reducing equivalents are provided by a single complex, leading to recovery of at least 90% of the complex as the undamaged $M(tpy)(bpy)OH_2^{2+}$ complex.[16] As seen in Table 4, *DNA catalyzes the self-inactivation process by over an order of magnitude*. Apparently, the catalyzed self-inactivation rate is too fast for DNA oxidation to be competitive, i.e. $k_X \gg k_{cleavage}$.

In addition to demonstrating that DNA is capable of catalyzing self-inactivation in general, we were interested in determining whether this catalysis was sequence-specific. The $Os(tpy)(bpy)O^{2+}$ complex was also treated with the polymers poly(dA)·poly(dT) and poly(dG)·poly(dC), and the kinetics of these reactions were investigated. The rate enhancements obtained at $R = 10$ are shown in Table 5. The rate constant for poly(dG)·poly(dC) was somewhat slower than that for calf thymus DNA; however, the rate constant is more than three times faster for poly(dA)·poly(dT) than for calf thymus DNA. Thus, *the sequence of the polymer influences the degree of catalysis of self-inactivation by DNA.*

Discussion

Redox Mechanisms. Comparison of the DNA chemistry of $Os(tpy)(bpy)O^{2+}$, $Ru(tpy)(bpy)OH^{2+}$, and $Ru(tpy)(bpy)O^{2+}$ offers a unique opportunity to study three structurally identical cleavage agents with significantly different reactivities. The difference in reactivity is evident in the redox potentials corresponding to the individual one-electron/one-proton oxidations (eqs 2 and 3). The potentials for ruthenium are $E_{1/2}(III/II) = 0.49$ V (eq 2) and $E_{1/2}(IV/III) = 0.62$ V (eq 3) at pH 7, and the corresponding potentials for osmium are 0.09 and 0.41 V, respectively.[17] Thus, for the $M^{IV}O^{2+}$ forms, the ruthenium complex is a better oxidant by about 200 mV, and the $Ru^{III}OH^{2+}$ complex is about 80 mV stronger than $Os^{IV}O^{2+}$. In addition, the $Os^{III}OH^{2+}$ complex is much more stable relative to the $Os^{II}OH_2^{2+}$ state than the ruthenium analogue, leading to a larger splitting of the IV/III and III/II couples for osmium. As a result, $Ru^{IV}O^{2+}$ is considerably better suited to two-electron oxidations, such as hydride transfers and oxo transfers,[22] than $Os^{IV}O^{2+}$ or $Ru^{III}OH^{2+}$.

Since the potentials of $Ru^{III}OH^{2+}$ and $Os^{IV}O^{2+}$ are similar and both are one-electron oxidants, both complexes might be expected to show similar reactivity. Indeed, both complexes are thermodynamically suited to hydrogen atom abstraction by addition of one electron and one proton to form $Ru^{II}OH_2^{2+}$ or $Os^{III}OH^{2+}$; however, Thompson and Meyer have shown that hydrogen atom abstraction from 2-propanol is three orders of magnitude slower than the analogous pathway for $Ru^{IV}O^{2+}$.[40] Hydrogen abstraction by $Ru^{III}OH^{2+}$ might therefore be too slow to compete with self-inactivation and guanine oxidation. In fact, the ability of $Ru^{III}OH^{2+}$ to oxidize DNA is probably related to the access of the $Ru^{IV}O^{2+}$ state via an unfavorable disproportionation:

$$2Ru^{III}OH^{2+} \rightleftharpoons Ru^{IV}O^{2+} + Ru^{II}OH_2^{2+} \quad (4)$$

The equilibrium constant for disproportionation is 0.050,[47] but efficient guanine oxidation by $Ru^{IV}O^{2+}$ could allow for some reaction to occur.

The mechanism of self-reduction of $Ru(tpy)(phen)O^{2+}$ has been studied in detail by Meyer and co-workers,[16] and the related mechanism of self-reduction of $Ru(bpy)_3^{3+}$ has been elucidated by Creutz and Sutin.[45,46] In the case of $Ru(bpy)_3^{3+}$, the rate-limiting step at high pH is addition of hydroxide to the ortho position on the pyridyl ring to yield a $[(bpy)_2Ru^{III}(bpyOH^-)]^{2+}$ complex.[46] This complex undergoes rapid intramolecular electron transfer to yield a bpyOH· radical:

$$[(bpy)_2Ru^{III}(bpyOH^-)]^{2+} \rightarrow [(bpy)_2Ru^{II}(bpyOH^\bullet)]^{2+} \quad (5)$$

This species is then oxidized by a second equivalent of $Ru(bpy)_3^{3+}$:

$$[(bpy)_2Ru^{II}(bpyOH^\bullet)]^{2+} + Ru(bpy)_3^{3+} \rightarrow [(bpy)_2Ru^{II}(bpyOH)]^{2+} + Ru(bpy)_3^{2+} \quad (6)$$

The resulting $[(bpy)_2Ru(bpyOH)]^{2+}$ complex is susceptible to further oxidation, so a large fraction of the original $Ru(bpy)_3^{2+}$ is recovered at the end of the reaction. The self-reduction of $Ru(tpy)(phen)O^{2+}$ and $ReO_2(py)_4^{2+}$ follow related mechanisms.[16,48] At neutral pH, the rate of decomposition of oxidized polypyridyl complexes has been shown to exhibit a complex dependence on the concentration of the metal complex with faster rates observed at higher metal complex concentrations.[45] Thus, at neutral pH, concentration of the metal complex by condensation on the DNA strand would be expected to enhance the rate of self-inactivation. These earlier mechanistic experiments were performed for $Ru(tpy)(phen)O^{2+}$ and $Ru(bpy)_3^{3+}$, and a detailed study of the inactivation of $Os(tpy)(bpy)O^{2+}$ itself now seems warranted.

Mechanism of Catalysis of k_X. Addition of DNA to a solution of $Os(tpy)(bpy)O^{2+}$ leads to an enhancement in the rate of self-reduction of a factor of 10–20. This degree of enhancement is consistent with simple condensation of the metal

(45) Creutz, C.; Sutin, N. *Proc. Natl. Acad. Sci. U.S.A.* **1975**, *72*, 2858–2862.
(46) Ghosh, P. K.; Brunschwig, B. S.; Chou, M.; Creutz, C.; Sutin, N. *J. Am. Chem. Soc.* **1984**, *106*, 4772–4783.
(47) Thompson, M. S.; Meyer, T. J. *J. Am. Chem. Soc.* **1982**, *104*, 5070. Binstead, R. A.; Stultz, L. K.; Meyer, T. J. *Inorg. Chem.* **1995**, *34*, 546–551.
(48) Brewer, J. C. Thesis, California Institute of Technology, 1990.

Scheme 3

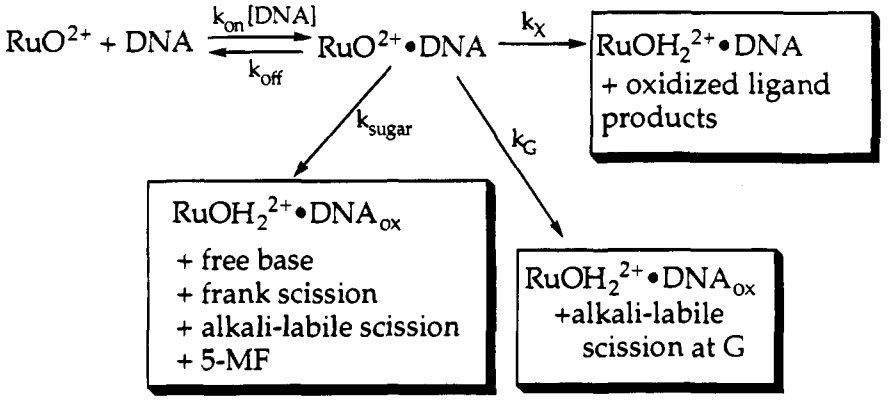

complexes on the DNA strand and an increased effective concentration of partners in a bimolecular reaction. If this were the mechanism, we would expect to see second-order decays in the presence of DNA. The failure to observe second-order kinetics probably stems from the complex nature of the decomposition reaction[45] and the low extent of binding of the complex, which would make changes in the decay between DNA and solution difficult to discern. Bimolecular electron-transfer reactions between complexes of similar affinity show rate enhancements on the same order under similar conditions of DNA and metal complex concentration, and in these cases, decays remain first order and Stern–Volmer plots remain linear.[49,50] In addition, a GpG binding site for a cationic platinum complexe is labeled more rapidly when included in longer oligonucleotides,[51] and this effect also arises from electrostatic condensation of cationic complexes on the DNA polymer.

Thus, the rate enhancement is simply a function of the binding of the metal complex to DNA. In this case, the sequence specificity should reflect the difference in binding affinity of the metal complex for the particular sequence. Relatively small differences in binding affinity are difficult to measure for complexes with very weak affinities, such as Os(tpy)(bpy)-OH_2^{2+}; however, it has been shown on numerous occasions that the affinities for related complexes are greater for AT sequences and regions. For example, Barton et al. have reported the affinities of $Ru(phen)_3^{2+}$ for poly(dA)·poly(dT) (K_b = 9200 M^{-1}), calf thymus DNA (K_b = 6200 M^{-1}), and poly(dG)·poly-(dC) (K_b = 4000 M^{-1}).[52] These affinities follow the same trend (AT > DNA > GC) as the rate enhancements for the self-reduction of $Os(tpy)(bpy)O^{2+}$ shown in Table 5. In addition, a complex like $Os(tpy)(bpy)O^{2+}$ is expected to bind solely by electrostatics, which has been demonstrated rigorously for the ruthenium analogue.[24] Electrostatic binding is much more favorable in the minor groove than the major groove because the anionic phosphates are in closer proximity,[53] and the observations here of 1′ oxidation and competition by distamycin strongly implicate binding of the complex in the minor groove.[5,30,32] Furthermore, electrostatic binding in the minor groove is more favorable for AT base pairs, because of the presence of the electropositive amino group in the minor groove of GC base pairs.[53] This consideration also indicates more favorable binding of the metal complex to poly(dA)·poly-(dT), which is consistent with our analysis of the kinetic data in Table 5.

Cleavage Mechanism. We can now view the cleavage reaction broadly using the model shown in Scheme 3. Binding of $Ru^{IV}O^{2+}$ to DNA occurs via a weak binding equilibrium with K_b = 660 M^{-1}. Even though this implies a relatively fast k_{off}, our earlier kinetic studies demonstrated that the metal complex is always reduced prior to dissociation.[14] Reduction of the bound complex therefore occurs via partitioning between three pathways: sugar oxidation, guanine oxidation, and self-inactivation. The results in Figure 2 show that the yield of oxidation at guanine is 7 times that at the other nucleotides. Since we know that the yield of base release is 10% based on total ruthenium,[15] we should be able to estimate the number of oxidizing equivalents consumed through guanine oxidation. Base release experiments show that the amount of guanine released is similar to the amounts of adenine, thymine, and cytosine released. Thus, some of the cleavage at G arises from sugar oxidation. By making the assumption that the extent of sugar cleavage at G is equal to that at A, T, and C, we can estimate that the yield of guanine oxidation is 6 times that of sugar oxidation at each nucleotide. Since all four nucleotides can react by sugar oxidation, the relative yield of base oxidation would be 1.5 times that of sugar oxidation. Thus, if sugar oxidation consumes 10% of the total ruthenium, base oxidation consumes an additional 15%.

By estimating the yields of both sugar and base oxidation, we can account for about 25% of the total ruthenium based on $Ru(tpy)(bpy)O^{2+}$ based on a two-electron process. However, we have shown previously that the DNA oxidations occur in two stages.[11,14] The first stage involves oxidation by $Ru^{IV}O^{2+}$ to generate $Ru^{II}OH_2^{2+}$:

$$Ru^{IV}O^{2+} + DNA \rightarrow Ru^{II}OH_2^{2+} \quad (7)$$

Once $Ru^{II}OH_2^{2+}$ is produced, comproportionation occurs to generate $Ru^{III}OH^{2+}$:

$$Ru^{IV}O^{2+} + Ru^{II}OH_2^{2+} \rightarrow 2Ru^{III}OH^{2+} \quad (8)$$

The second stage of the reaction involves the much slower reduction of $Ru^{III}OH^{2+}$ to $Ru^{II}OH_2^{2+}$:

$$Ru^{III}OH^{2+} + DNA \rightarrow Ru^{II}OH_2^{2+} \quad (9)$$

These same stages have been observed in oxidations of small molecules.[40] Thus, only half of the starting $Ru(tpy)(bpy)O^{2+}$ reacts from the $Ru^{IV}O^{2+}$ state, because the other half is used to

(49) Orellana, G.; Kirsch-De Mesmaeker, A.; Barton, J. K.; Turro, N. J. *Photochem. Photobiol.* **1991**, *54*, 499–509.
(50) Barton, J. K.; Kumar, C. V.; Turro, N. J. *J. Am. Chem. Soc.* **1986**, *108*, 6391–6393.
(51) Elmroth, S. K. C.; Lippard, S. J. *J. Am. Chem. Soc.* **1994**, *116*, 3633–3634.
(52) Barton, J. K.; Goldberg, J. M.; Kumar, C. V.; Turro, N. J. *J. Am. Chem. Soc.* **1986**, *108*, 2081–2088.
(53) Jayaram, B.; Sharp, K. A.; Honig, B. *Biopolymers* **1989**, *28*, 975–993.

generate $Ru^{III}OH^{2+}$ via eq 8. The base release measurements[14] and the sequencing gel experiments in Figure 2 are performed after all of the $Ru^{IV}O^{2+}$ has been reduced but long before an appreciable amount of $Ru^{III}OH^{2+}$ has been reduced. The kinetic measurements show conclusively that eq 7 is over in a few minutes while completion of eq 9 requires hours.[14] Thus, a yield of 25% of DNA oxidation based on $Ru(tpy)(bpy)O^{2+}$ actually corresponds to a yield of 50% when the comproportionation reaction (eq 8) is considered along with the fact that DNA cleavage is a two-electron oxidation.

An accounting of half of the oxidizing equivalents based on $Ru(tpy)(bpy)O^{2+}$ implies that about 50% of the total $Ru^{IV}O^{2+}$ reacts via the k_X pathway, which we cannot observe explicitly for $Ru^{IV}O^{2+}$ but can observe explicitly for $Os^{IV}O^{2+}$. Thus, our observations imply that in terms of Scheme 3, $k_X > k_G > k_{sugar}$ for $Ru^{IV}O^{2+}$. This ordering makes the prediction that a less powerful oxidant will be reduced via the k_X and k_G pathways, but not via k_{sugar}, as long as the rates of the various processes are directly related to the thermodynamic driving force. This prediction is confirmed by the results on $Ru^{III}OH^{2+}$, which clearly show that some base oxidation still occurs but no sugar oxidation is realized. The rate of k_X compared to k_G must also be increased since densitometry shows that the yield of base oxidation from $Ru^{III}OH^{2+}$ is only 14% of that realized with $Ru^{IV}O^{2+}$. Finally, the further prediction can be made that an even weaker oxidant than $Ru^{III}OH^{2+}$ should be reduced efficiently in the presence of DNA with no detectable damage to the nucleic acid, i.e. only the k_X pathway is operative. This prediction is confirmed by the results on $Os^{IV}O^{2+}$.

Another very interesting point brought out by the results in Figures 2 and 3 is the observation of the same chemical mechanism for both duplex and single-stranded DNA. The formation of the same 3′-modified phosphate termini (**3**) and only 5′-phosphate termini strongly supports 1′ oxidation in both cases. In fact, recent studies in our laboratory suggest that only 1′ oxidation occurs with $Ru(tpy)(bpy)O^{2+}$ in simple mononucleotides and sugars,[28] and we have made parallel observations for photoreactions of $Pt_2(pop)_4^{4-}$.[54] A recent theoretical study shows that the 1′ carbon in deoxyribose is indeed the thermodynamically favored position for hydrogen abstraction.[55] Thus, it appears that the selection of a particular position for hydrogen abstraction is based on the relative thermodynamic driving force for the reaction. This behavior is in contrast to that seen in many other oxidants, such as bleomycin and the enediynes, which apparently select hydrogens for abstraction based on accessibility and the configuration of the drug−DNA adduct.[5,32,56] The $Ru(tpy)(bpy)O^{2+}$ complex is a much weaker oxidant than high-valent iron or benzene diradical and is therefore more likely to select based on thermodynamic facility.

Our kinetic results on the reduction of $Os^{IV}O^{2+}$ clearly show that k_X is catalyzed by DNA for this particular oxidant. For the $Ru^{IV}O^{2+}$ experiments, we cannot show directly that this pathway is catalyzed relative to homogeneous solution. However, inspection of the relative yields of oxidation in DNA and in homogeneous oxidations of small molecules reveals that catalysis must occur. Oxidation of substrates such as 2-propanol and activated hydrocarbons proceeds in many cases with quantitative yields of oxidized products based on total $Ru^{IV}O^{2+}$ (or on applied current in electrolytic oxidations).[57] Thus, a conversion of only 50% of the total $Ru^{IV}O^{2+}$ into DNA oxidation implies that self-inactivation competes much more effectively with substrate oxidation in DNA than in homogeneous solution. This implies either that DNA catalyzes the self-inactivation or that the substrate oxidation is much slower in the polymer. Based on our observations on $Os^{IV}O^{2+}$, catalysis of k_X seems more likely, especially in single-stranded oligomers where a complex structure is not likely to obstruct oxidation sites.

Implications. A final question involves how these results on the $M(tpy)(bpy)O^{2+}$ systems impact on nucleic acid oxidation by other cleavage agents, such as Cu-phen[30] and FeBLM.[4,5] The first point raised is whether these agents also partition between base and sugar oxidation. With small molecules, $Ru(tpy)(bpy)O^{2+}$ and FeBLM are both broad-spectrum oxidants.[5,57] In particular, all three complexes are excellent agents for the conversion of styrene to styrene oxide,[58−60] which is certainly a more difficult oxo transfer reaction than the oxidation of guanine to 8-oxoguanine. Further, the results here show that guanine oxidation is both kinetically and thermodynamically favored over sugar oxidation, and both Cu-phen and FeBLM are excellent agents for sugar oxidation. There are a few reports of guanine oxidation observed from Cu-phen cleavage reactions;[61,62] however, there is no evidence of which we are aware that implicates guanine oxidation by FeBLM, even in RNA's with significant numbers of guanines in single-stranded regions.[63] Since both Cu-phen and FeBLM are certainly capable agents for guanine oxidation, the failure to observe the significant levels of guanine oxidation observed with $Ru(tpy)(bpy)O^{2+}$ must arise from the geometric aspects of the oxidants. Burrows et al. have shown convincingly that guanine oxidation is strongly dependent on the accessibility of the guanine base to solvent,[27,29,64] so subtle differences in the accessibility of the reactive oxo group in the oxidant may modulate the guanine reactivity. This idea suggests that we may be able to develop oxidants based on $Ru(tpy)(bpy)O^{2+}$ that are selective for base or sugar oxidation by systematically varying the ligand environment and the oxo ligand accessibility.

A second point raised is the potential relevance of the sequence-specific catalysis of k_X to cleavage by other agents. In particular, while our results do not bear directly on any experiments involving FeBLM, we have shown that k_X can indeed be sequence specific, at least in the $Ru(tpy)(bpy)O^{2+}$ system. This finding can now be considered in light of the suggestion of Worth et al. that sequence-specific isotope effects can arise from a sequence dependence of the dynamics of other reaction pathways via eq 1.[9] The results reported here support the suggestion that the sequence-specific isotope effects for FeBLM could be a result of sequence specificity in k_X. Of course, only further experimentation on FeBLM itself will reveal which mechanism is operative.

Finally, the overall implications of the catalysis of k_X by DNA must be considered. As discussed earlier, catalysis of reactions

(54) Kalsbeck, W. A.; Gingell, D. M.; Malinsky, J. E.; Thorp, H. H. *Inorg. Chem.* **1994**, *33*, 3313−3316.
(55) Miaskiewicz, K.; Osman, R. *J. Am. Chem. Soc.* **1994**, *116*, 232−238.
(56) Mah, S. C.; Townsend, C. A.; Tullius, T. D. *Biochemistry* **1994**, *33*, 614−621.
(57) Thompson, M. S.; DeGiovani, W. F.; Moyer, B. A.; Meyer, T. J. *J. Org. Chem.* **1984**, *49*, 4972.
(58) Murugesan, N.; Hecht, S. M. *J. Am. Chem. Soc.* **1985**, *107*, 493−500.
(59) Heimbrook, D. C.; Mulholland, R. L.; Hecht, S. M. *J. Am. Chem. Soc.* **1986**, *108*, 7839−7840.
(60) Dobson, J. C.; Seok, W. K.; Meyer, T. J. *Inorg. Chem.* **1986**, *25*, 1513−1514.
(61) Shimizu, M.; Inoue, H.; Ohtsuka, E. *Biochemistry* **1994**, *33*, 606−613.
(62) Aruoma, O. I.; Halliwell, B.; Gajewski, E.; Dizdaroglu, M. *Biochem. J.* **1991**, *273*, 601−604.
(63) Holmes, C. E.; Hecht, S. M. *J. Mol. Biol.* **1993**, *268*, 25909−25913.
(64) Chen, X.; Woodson, S. A.; Burrows, C. J.; Rokita, S. E. *Biochemistry* **1993**, *32*, 7610−7616.

of cations bound to DNA has been observed for bimolecular electron-transfer reactions and labeling of guanine by platinum.[49,51,65,66] We report here that DNA is also able to catalyze the self-inactivation of a series of oxidizing metal complexes. In this way, the DNA is effectively protecting itself from damage. Furthermore, the sequence specificity implies that different sites on DNA can protect themselves from damage to different degrees, because sites that promote k_X more effectively are less likely to be oxidized. This concept potentially provides a new route to selective DNA oxidation that is not based on a binding or shape-selection mechanism[2,67-69] or a simple accessibility mechanism.[3,27,29,56,64,70] In contrast, an additional route to specificity in cleavage could arise from differences in the ability of individual sites to catalyze k_X and thereby protect themselves from oxidation.

Acknowledgment. We thank S. Poteat and Dr. N. Grover for experimental assistance. H.H.T. thanks the National Science Foundation for a Presidential Young Investigator Award and the David and Lucile Packard Foundation for a Fellowship in Science and Engineering. T.W.W. thanks the Department of Education for a Graduate Fellowship.

Supplementary Material Available: GC-MS data for detection of **4**, the agarose gel showing conversion of form I to form II plasmid DNA by $Os(tpy)(bpy)O^{2+}$, and a polyacylamide gel showing the effect of oxygen on the cleavage reaction, tables giving complete interatomic distances and angles, and a drawing of $[Os(tpy)(bpy)OH_2](CF_3SO_2)_2$ showing the complete atomic labeling (10 pages); a listing of observed and calculated structure factors (20 pages). This material is contained in many libraries on microfiche, immediately follows this article in the microfilm version of the journal, can be ordered from the ACS, and can be downloaded from the Internet; see any current masthead page for ordering information and Internet access instructions.

JA942769F

(65) Murphy, C. J.; Arkin, M. R.; Jenkins, Y.; Ghatlia, N. D.; Bossmann, S. H.; Turro, N. J.; Barton, J. K. *Science* **1993**, *262*, 1025-1029.
(66) Purugganan, M. D.; Kumar, C. V.; Turro, N. J.; Barton, J. K. *Science* **1988**, *241*, 1645-1649.
(67) Campisi, D.; Morii, T.; Barton, J. K. *Biochemistry* **1994**, *33*, 4130-4139.
(68) Pyle, A. M.; Morii, T.; Barton, J. K. *J. Am. Chem. Soc.* **1990**, *112*, 9432.
(69) Pyle, A. M.; Long, E. C.; Barton, J. K. *J. Am. Chem. Soc.* **1989**, *111*, 4520.
(70) Tullius, T. D.; Dombroski, B. A. *Science (Washington, D.C.)* **1985**, *230*, 679.